Lawrence Berkeley National Laboratory
LBL Publications

Title
Atomic layer etching of SiO2 with Ar and CHF 3 plasmas: A self-limiting process for aspect ratio independent etching

Permalink
https://escholarship.org/uc/item/4cn657t1

Journal
Plasma Processes and Polymers, 16(9)

ISSN
1612-8850

Authors
Dallorto, Stefano
Goodyear, Andy
Cooke, Mike
et al.

Publication Date
2019-09-01

DOI
10.1002/ppap.201900051

Peer reviewed

eScholarship.org Powered by the California Digital Library
University of California

Article type: Full Paper

Atomic Layer Etching of SiO_2 with Ar and CHF_3 Plasmas: a Self-Limiting Process for Aspect Ratio Independent Etching

Stefano Dallorto, Andy Goodyear, Mike Cooke, Julia E. Szornel, Craig Ward, Christoph Kastl, Adam Schwartzberg, Ivo W. Rangelow, Stefano Cabrini*

S. Dallorto, I. W. Rangelow
Ilmenau University of Technology, Dept. of Micro- and Nanoel. Syst., 98684, Germany

S. Dallorto, A. Goodyear, M. Cooke, C. Ward
Oxford Instruments Plasma Technology, North End, Yatton, Bristol BS49 4AP, United Kingdom

S. Dallorto, J. E. Szornel, A. Schwartzberg C. Kastl, S Cabrini
Molecular Foundry, Lawrence Berkeley National Laboratory, Berkeley, 94720, United States
E-mail: scabrini@lbl.gov

With ever increasing demands on device patterning to achieve smaller critical dimensions, the need for precise, controllable atomic layer etching is steadily increasing. In this work, a cyclical fluorocarbon/argon plasma is successfully used for patterning silicon oxide by atomic layer etching in a conventional inductively coupled plasma tool. The impact of plasma parameters and substrate electrode temperature on the etch performance is established. We achieve self-limiting behavior of the etch process by modulating the substrate temperature. We find that at a electrode temperature of -10 °C, etching stops after complete removal of the modified surface layer as the desorption of adsorbed fluorine radicals from the reactor walls into the plasma is minimized. Lastly, we demonstrate the ability to achieve ndependent etching, which establishes the potential of

the developed cyclic atomic layer etching process for small scale device patterning.

1 Introduction

Advanced nanomanufacturing is increasingly demanding atomic-scale process controllability to produce features with sub-10 nm critical dimensions.[1, 2] The performance of the resultant devices depends critically on the etching step, presenting etch challenges that continue to increase as process requirements grow more stringent.[3, 4] The necessary control of surface properties in combination with the decrease in overall film thicknesses require material selectivity and atomic scale control of etching directionality at the truly atomic scale.[5] Atomic Layer Etching (ALE) offers this level of control of etch performance, and has significant potential to overcome the challenges confronting modern nanofabrication techniques. The ALE process consists of two sequential steps: first, the surface of the material is chemically modified creating a thin reactive surface layer with well-defined, angstrom-scale thickness. Second, in the etch step, the modified surface layer is selectively removed by bombardment with Ar ions. The ions used during the etch step induce a chemical reaction between the absorbed species and the substrate. Importantly, physical ion bombardment allows for the directional etching required to generate high aspect ratio nanoscale features.

The separation of the chemical modification and subsequent etch steps enable the fluxes of neutral and charged particles to be independently optimized, despite their different transport methods.[6] By providing the ability to control the parameters of both charged and neutral particles independently, this process increases the accessible parameters space to include, for example, species fluxes and their relative ratios. The greatest benefit from ALE is achieved when both reactions, the chemical modification step and the etch step, are fully self-limiting. The use of self-limiting reactions allows for tolerance to over-exposure, which improves uniformity on length scales spanning orders of magnitude.

The reported ALE process also allows to reach aspect ratio independent etching (ARIE), which refers to the independence of vertical etch rate on the aspect ratio of the features being etched.[7, 8] Additionally, by taking advantage of the surface selectivity of the plasma chemistry, ALE also offers reduced surface damage and an uncommon substrate specificity.[5, 9] Over the past decade, ALE has been realized for a variety of materials including but not limited to Si, SiO_2, Si_3N_4, Al_2O_3, and HfO_2.[6, 10-14]

SiO_2 is one of the most important materials in semiconductor nanofabrication.[15] The mechanism behind continuous etching of SiO_2 has been widely studied.[3, 16] Selective etching of SiO_2 over Si and Si_3N_4 can be performed in inductively coupled plasma (ICP) using fluorocarbon plasmas, and the etch rate is inversely proportional to the thickness of the fluorocarbon (FC) film deposited on the surface.[17, 18] Computational investigation of plasma assisted ALE of SiO_2 showed that when the plasma chemistry and plasma ion energies during each step are controlled, it is possible to reach a self-limiting etching process.[9] ALE of SiO_2 was then

evaluated using cycles of inductively coupled Ar and fluorocarbon plasmas.[19]

ALE of SiO_2 with fluorocarbon plasmas is realized by passivating the surface with an angstrom-thin fluorocarbon layer followed by Ar ion etching. The fluorocarbon layer lowers the binding energy of the SiO_2 surface atoms with the underlying lattice, creating an energy window where incoming Ar ions can sputter the modified surface layer, but do not have enough energy to remove pristine SiO_2 sites. [20, 21] Here, we develop a self-limiting ALE process of SiO_2 using fluoroform (CHF_3). To avoid the use of specialized equipment, which is also undesirable from a cost perspective, we have optimized the process for use in a conventional ICP tool.[22] We first investigated the etch step using low energy Ar ion bombardment. In a plasma environment, the ion energy distribution controls the physical sputtering and the extent of damage to the substrate. By carefully tailoring the ion bombardment energy via the forward bias plasma power (RF power), we demonstrate control of the etching depth per cycle (EPC), reaching a self-limiting behavior. We also found that the substrate temperature critically controls this self-limiting behavior. We showed that the amount of fluorocarbon polymer formed on the SiO_2 increases as the substrate temperature is reduced, ultimately controlling the etch step. The gradual change in the self-limiting EPC is due to the residual fluorine radicals in the ICP chamber that are released during the Ar bombardment. Ultimately, we show that self-limiting and aspect-ratio independent ALE is achieved combining a substrate temperature of -10 °C and low forward bias power.

2 Experimental Section

2.1 Experimental apparatus and plasma analysis

All work was performed using a Plasmalab System 100 ICP etcher from Oxford Instruments Plasma Technology. In a typical process, the wafers are loaded into the chamber via a load-lock and mechanically clamped to a temperature-controlled substrate holder. The substrate electrode was cooled with liquid nitrogen, allowing precise control of the substrate temperature from -150 °C to 400 °C. The chamber wall temperature was fixed at 60 °C. Radio frequency (RF) power (13.56 MHz) was applied to the ICP source (up to 3000 W) and the substrate electrode (up to 500 W) to generate the plasma. The RF power supplied by the substrate electrode generates a DC bias that controls the ion energy at the substrate.

Plasma parameters, including ion energy distribution (IED) and total ion flux were measured using a commercial retarding field energy analyzer (RFEA) Semion™ System 500. The sensor was mounted on a 4-inch Si wafer, with the front face parallel to the lower electrode surface, perpendicular to the direction of ion travel. The analyzer was biased with a potential sweep to discriminate Ar ions with different energies. The IED was determined from the ion-current characteristic, while the ion flux was determined by integrating the measured IED. The complete description of the analyzer is reported elsewhere.[23, 24]

2.1 Fluorocarbon ALE

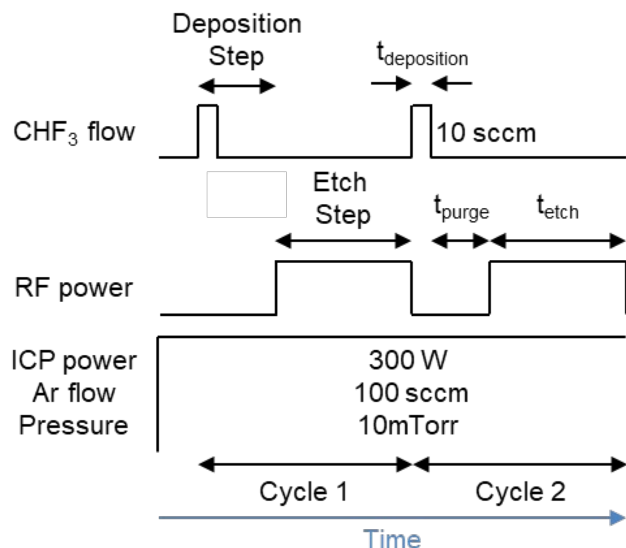

Figure 1. Schematic of fluorocarbon based ALE. The ALE experiment was conducted with a continuous, steady-state Ar plasma and repeated ALE cycles. Each cycle consists of a fluorocarbon polymer deposition step and a low energy ion bombardment etch step. The deposition step is unbiased (RF power off), and starts with a short CHF_3 injection followed by a chamber purge. The etch step is biased (RF power on), and its duration (etch time) was varied to optimize self-limiting behavior.

We used Si substrates with 100 nm of thermally grown SiO_2 to develop the ALE process. The SiO_2 test samples (0.5 x 1 in^2) were positioned on 4-inch Si carrier wafers and kept in place using Fomblin oil, which granted mechanical stability and improved the thermal contact and between sample and carrier. To establish consistent process parameters, the samples were loaded after a chamber cleaning and conditioning procedure comprised of an oxygen plasma cleaning followed by an Ar plasma preconditioning and 30 cycles of the main ALE process. We used spectroscopic ellipsometry (UVISEL, Horiba) to quantify the extent of material modification and etch depth. For unpatterned SiO_2 on Si substrates, the ellipsometry data was fitted using a two-layer optical

model, which consists of a fixed bottom Si layer and a varying top layer. The top layer represents a combination of SiO_2, fluorinated SiO_2 (mixed layer), and fluorocarbon. This optical model provides a good approximation of the data since the optical properties of the FC layer, the mixed layer, and the SiO_2 layer are similar.[25] The small differences in refractive indices of the FC and mixed layers are dwarfed by the large differences in thickness between the fluorocarbon (angstroms) and the SiO_2 layer (10 nm).

Figure 1 shows a schematic ALE process sequence. During the entire process, there was continuous Ar flow at 100 sccm. The chamber pressure was held at 10 mTorr, and the ICP power held constant at 300 W. For the deposition half-cycles, short periodical injections of 10 sccm of CHF_3 were introduced. The injection time ($t_{deposition}$) was varied to achieve the desired deposition thickness. We found that for $t_{deposition}$ = 3 s the mass flow controllers (MFC) produce a stable and reproducible fluorocarbon injection. After the CHF_3 pulse, a purging step (t_{purge} = 30 s) with pure Ar plasma ensures that all the fluorocarbon compounds are exhausted from the process chamber. The deposition and purge steps were unbiased (0 V DC bias). During the etch half-cycle, RF power was applied to generate a DC bias in the range of 0-50 V. Powered electrodes caused the Ar ions to be accelerated toward the SiO_2 with low ion energy. Different etch step lengths (etch time or t_{etch}) were also explored.

3 Results and Discussion

3.1 Plasma Diagnostic for ALE

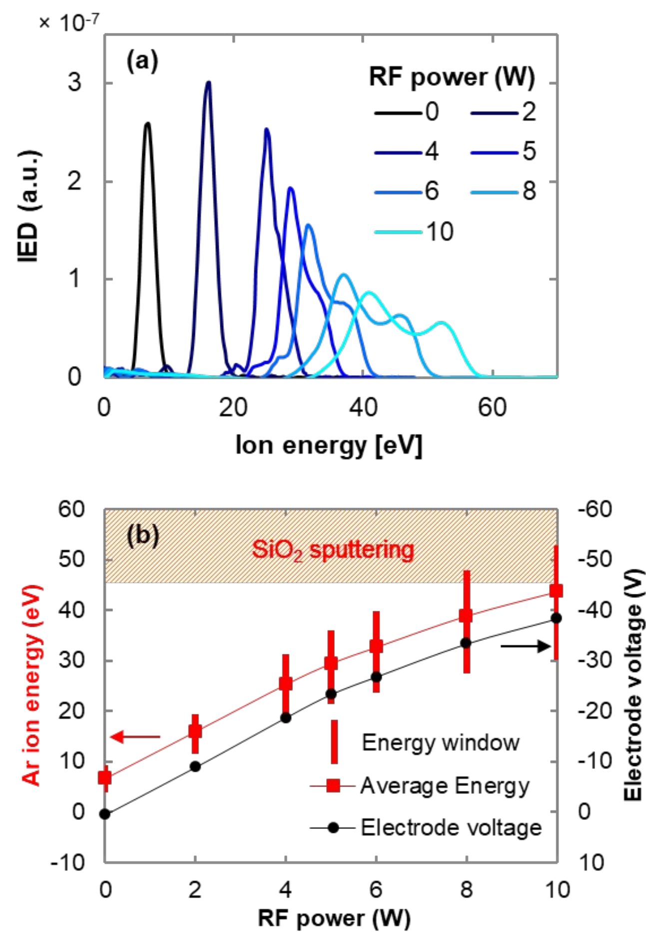

Figure 2. (a) Measured ion energy distribution (IED) for different values of the RF bias applied to the lower electrode. Experimental parameters are 10 mTorr chamber pressure, 300 W ICP power, and 100 sccm Ar flow. (b)

Measured electrode voltage (DC bias) and average energy of the measured IED function as a function of the discharge power. The error bars quantify the width of the distribution. They denote the energy window comprising 98% of the integrated area of the IED.

Self-limiting surface reactions are required to control the etch depth per cycle independently of etching time. To achieve true ALE etching, both spontaneous chemical etching during the deposition step and physical sputtering of unmodified SiO_2 during the etch step should be minimized. In the deposition step, the CHF_3 pulse in followed by a purging step where any CHF_3 residual is evacuated from the chamber. After the deposition step, the fluorocarbon layer reacts with the substrate surface below, lowering the threshold energy necessary to remove material from the surface compared to pristine SiO_2. The nature of the interaction of Ar ions with surface species is in part determined by the ion energy. Ar ions gain energy when they are accelerated through the plasma sheath, which in turn means that the Ar ions energy is proportional to the RF forward power. When the process parameters are adjusted such that the Ar ion energy is above the threshold for ion activated chemical sputtering of the FC-mixed layer, but still below the threshold for SiO_2 physical sputtering, it is possible to selectively remove the modified surface layer without damaging the underlying unmodified SiO_2. The ions from the plasma incident on the SiO_2 surface can have a broad energy distribution that dictates the physical sputtering rate and extent of substrate damage. To avoid this, careful adjustment of the Ar ion energy is instrumental in controlling the ALE process. Below, we demonstrate how the ion energy distribution of the ions impinging on the wafer can be adjusted by applying RF power to the substrate.

Figure 2(a) shows the measured integrated energy distribution (IED) of the Ar plasma as a function of RF power applied to the lower electrode. CHF3 evacuated… All experimental data presented were collected using pure Ar plasma with 300 W inductively coupled source power. When the electrode is grounded (0 W RF power), the ions accelerated from the bulk plasma to the electrode acquire an energy equal to the floating sheath potential. The IED exhibits a single peak with average ion energy of 7 eV. With increasing RF power, the IED shifts to larger values. At RF power of 4 W, a second peak starts to evolve in the IED. As the RF power is further increased the bimodal peak separation increases. At RF power of 10 W, the IED consist of two clearly discernable peaks at about 40 eV and 55 eV. This shape evolution of the IED will be crucial in the ALE processes. Even though the average ion energy **(Figure 2(b))** may be lower than the threshold for sputtering bare SiO_2 (45 eV), [11] the maximum energy of the IED can exceed this energy threshold. The average energy of the measured distribution function and the time averaged electrode voltage (often referred as electrode voltage or DC bias) are determined using the retarding field energy analyzer. These parameters are plotted in Figure 2(b) as a function of the RF forward power. The indicated error bars denote the energy distribution which comprises 98% of the area under the IED curve. In other words, 1% of the Ar ions in the plasma has an energy smaller than the lower error bars and 1% has an energy higher than the upper error bars. From this representation, we can conclude that the Ar plasmas with RF powers higher than 8 W (DC bias larger than -33 V) have significant contributions of ions with energies above the threshold for sputtering SiO_2 and must be avoided.

3.2 DC bias optimization

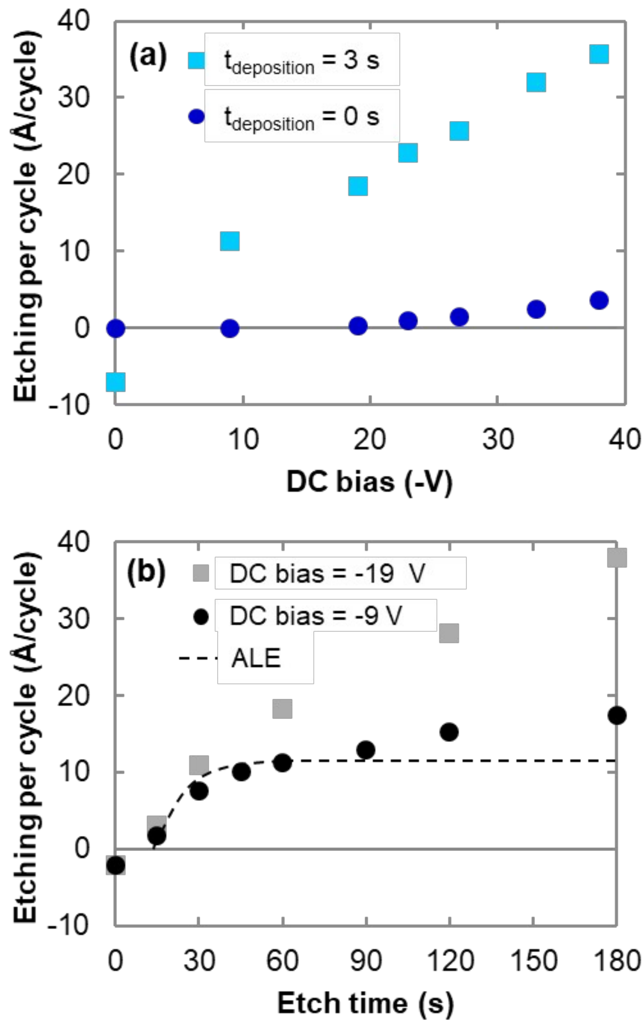

Figure 3. SiO_2 etching per cycle in a conventional PlasmaLab 100 ICP tool at 300 W ICP power, 10 mTorr pressure and 30 s purge. The substrate temperature is fixed at 20 °C. (a) SiO_2 etching per cycle vs DC bias, with ($t_{deposition}$ = 3 s) and without ($t_{deposition}$ = 0 s) the fluorocarbon dosing step. The etch time is fixed to 60 s. Without the chemical modification step no detectable etching of SiO_2 occurs for a DC bias smaller than 20 V. (b) SiO_2 etching per cycle vs etch time, for two DC bias values: 9 V and 19 V. Dose time is fixed to 3 s. In curve, "saturation curve" showing self-limiting removal in ALE.

The need for fine control of RF power is illustrated by **Figure 3(a)**, showing the SiO_2 removal when the Ar plasma was biased at different RF powers, both with ($t_{deposition}$ = 3 s) and without ($t_{deposition}$ = 0 s) fluorocarbon deposition step. The process without the fluorocarbon deposition step

corresponds simply to the sputtering rate of SiO_2 for different values of the DC bias. We find that at a DC bias below -19 V, no SiO_2 removal occurs. As the DC bias is increased above -19V, we observe sputtering of SiO_2. In particular, we observed a significant acceleration of this physical etching for DC bias higher than -33 V. At this voltage the IEDs exceed the SiO_2 sputtering window. However, even for DC bias of -23 V and -27 V, where the IED is nominally below the sputtering threshold of SiO_2, we detected a measurable sputtering rate. We understand this sputtering to be caused by very low concentrations of impurities in the substrate as the sputtering threshold is very sensitive to SiO_2 chemistry.[11] In turn, it is necessary to keep the DC bias below -19 V to avoid any ambient SiO_2 sputtering.

The introduction of a fluorocarbon surface modification is introduced via a 3 s CHF_3 gas pulse. This adsorbs the chemical reactant to SiO_2 (Figure 3(a), $t_{deposition}$ = 3 s), and allows the material to be etched with lower activation energy compared to the unmodified SiO_2.

One of the main advantages of ALE is the opportunity to separate the FC-SiO_2 chemical surface modification from the physical removal of the surface layer. Separation of reactions allows for the decoupling of the generation and transport of ions, electrons and radicals and facilitates self-limiting reactions[26]. Self-limiting reactions are reactions that slow down as a function of time. Here, etching takes place in an initial time followed by a removal rate that approaches zero. In **Figure 3(b)** we evaluated the amount of material etched per cycle when the etch step length is increased from 0 s to 180 s. At 0 s no SiO_2 etching is detected and a thin fluorocarbon film (3 Å thick) is deposited on the surface. The etch step is approaching a self-limiting regime when the DC power is reduced from -19

V to -9 V. For -9 V DC bias the EPC has the largest variation in the first 60 s, reaching 11 Å/cycle. A quasi-ALE behavior is observed, where the EPC does not completely saturate but slightly increases in the following 120 s. The need to reach complete saturation of SiO_2 EPC over etch time made us extend the study of SiO_2 ALE to different substrate temperatures.

3.3 Temperature control

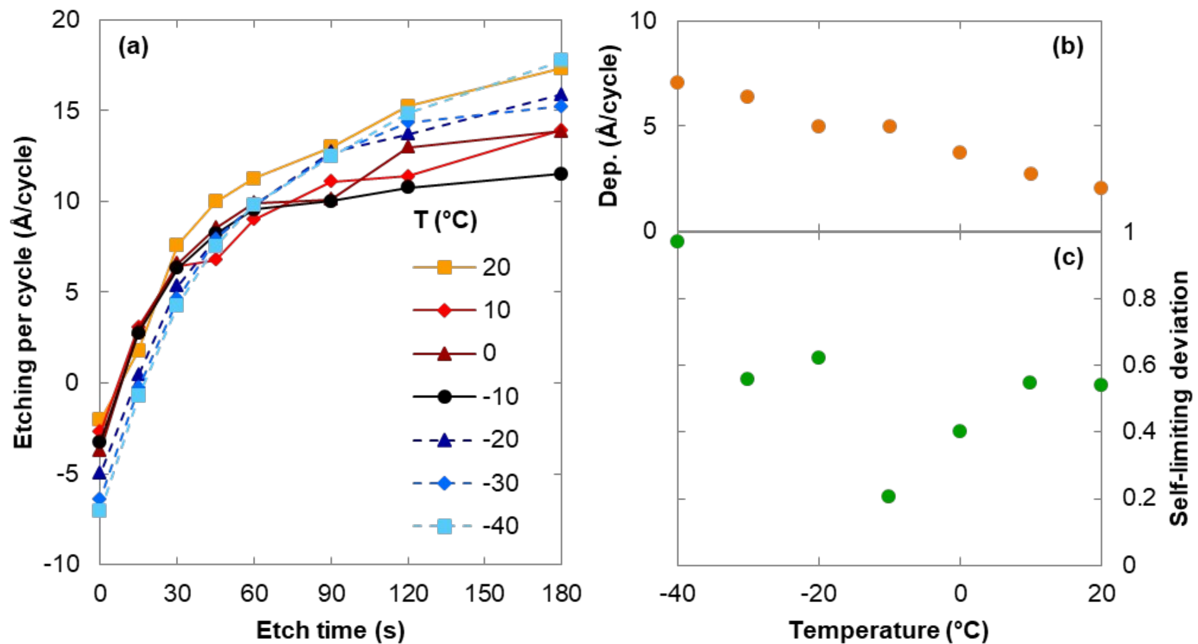

Figure 4. (a) SiO_2 thickness changes over Ar plasma etching time during one ALE cycle with varying substrate temperature, following fluorocarbon deposition of 3 s and purging the reactor chamber for 30 s. (b) Measured thickness of the fluorocarbon film deposited on SiO_2 during one ALE cycle as a function of the substrate temperature. (c) Deviation of the etch per cycle from self-limiting behavior defined as $(EPC(180\,s) - EPC(60\,s))/EPC(60\,s)$*. Self-limiting behavior of the etching is achieved for a substrate temperature of -10 °C.*

The substrate temperature significantly impacts the sticking coefficient of the FC polymer deposited on SiO_2. The sticking coefficient is expected to increase with decreasing temperature.[27] The deposition step is essential to establish ALE. To allow high aspect ratio etching of features with small critical dimension, the sidewall FC layer needs to be thin and penetrate deep into the feature. The importance of the FC sticking coefficient on SiO_2

is reinforced by the increase of FC deposition with decreasing temperature. **Figure 4(a)** shows the SiO_2 etching rate per cycle as a function of etch step time and temperature between 20 °C and -40 °C. Temperatures as low as -60 °C were also explored, but no substantial benefits were detected. The data collected at t_{etch} = 0 s have negative values and correspond to the FC deposition rate on the SiO_2 surface. The values for the FC film thickness deposited per cycle as a function of temperature are plotted in **Figure 4(b)**. Moving from room temperature to -40 °C, the deposition per cycle changed approximately linearly from 2 Å/cycle to 7 Å/cycle. The change in the FC deposition rates strongly impacts the curves in Figure 4(a).

Working in true ALE regime, the EPC vs etch time would show a self-limiting behavior, meaning that SiO_2 etching is happening in an initial "burst" but after consuming the FC film the etch stops and the EPC remains constant in value. For this reason, we defined a quantity that measures how much in percentage the curves in Figure 4(a) deviate from saturation after 60 s etching. This deviation from the self-limiting behavior was determined by calculating $\left[\frac{EPC(180\,s)-EPC(60\,s)}{EPC(60\,s)}\right]$ (100 %), where $EPC(t_{etch})$ is the etching per cycle of SiO_2 using an etch step of t_{etch} s. This quantity is calculated for each curve at different temperature and the results are plotted in **Figure 4(c)**.

As evidenced in Figure 4(c), etching per cycle approaches a self-limiting behavior at a substrate temperature of -10 °C. At this temperature the EPC after 60 s is 9.5 Å/cycles and for the following 120 s it only changes 20 %,

reaching a value of 11.5 Å/cycles. For temperatures different than -10 °C the curves in Figure 4(a) divert from self-limiting behaviors. From our data, we can conclude that the atomic layer etching of SiO_2 is subject to two different contributions that are minimized at -10 °C. For electrode temperatures higher than -10 °C, it is proposed that the etching rate increases because of residual fluorine in the chamber. Fluorine coming from the chamber walls and fluorocarbon polymer removed during the etch step are just two fruitful sources of residual fluorine in the ICP. Higher temperatures enhance SiO_2 chemical etching by fluorine.[28] This result was experimentally confirmed by first fluorinating the chamber walls with pure SF_6 plasma (50 sccm SF_6, 2000 W ICP, 0 V DC bias) and then running a pure Ar plasma (300 W ICP, -9 V DC bias). SiO_2 etching was evaluated during the pure Ar plasma. With clean chamber walls no SiO_2 etching was detected but when the chamber walls were fluorinated the Ar plasma etched the SiO_2 at a rate of was 9 Å/min, 0.5 Å/min, and 0 Å/min at substrate temperatures of 20 °C, -10 °C and -40 °C, respectively. This result proves the strong effect of substrate temperature on the chemical etching caused by residual fluorine radicals, but it also showed that for substrate temperatures lower than -10 °C the impact of fluorine contamination from the chamber walls on the etch process is negligible. In addition, continues etching of SiO_2 with fluorine shows an etch rate that increases strongly for increasing temperatures, suggesting an increase of reactivity between the FC film and the SiO_2 at high temperatures.[28,29] The FC layer deposition plays an opposite role. We know that the etching of SiO_2 occurs during the Ar ion bombardment phase when SiO_2 is converted to fluorinated-SiO_2 by mixing with FC polymer.[30] Since the

entire FC layer must be consumed during the etch step, the amount of SiO_2 etched is proportional to the initial polymer thickness. The reaction of the FC polymer with SiO_2 happens continuously during the Ar ion bombardment step with further FC-mixing reactions and hence SiO_2 removal happening throughout, until the polymer is fully depleted.[30] This results in an EPC that depends on polymer thickness, which in turn depends on electrode temperature. For high substrate temperatures, the FC layer deposited is thinner and the etching of SiO_2 terminates once all the polymer is consumed. For lower temperatures, thicker polymer is deposited during each cycle, and a longer etch time is needed to completely remove the fluorinated-SiO_2. This implies that the EPC curves at substrate temperatures below -10 °C may still reach saturation but at a higher EPC and at a longer etch time.

To summarize, for substrate temperature higher than -10 °C the SiO_2 EPC is affected by the residual fluorine radicals in the chamber walls, while for temperature lower than -10 °C the EPC is affected by the FC polymer. The two effects compensate at -10 °C showing a self-limiting behaviors after 60 s etch time and EPC of 10 Å/cycles is observed. Based on the evidence above we can reach ALE of SiO_2 but independently from the process there is always some residual fluorine in the chamber which limits the self-limiting behavior. These limitations raising from residual fluorine highlights the difficulties in finding the right parameters for reaching ALE. In conclusion, we identify the ALE at -10 °C as the best process and it is the one used for pattern transfer, as described in the following section.

3.4 SiO_2 patterning using FC-based ALE

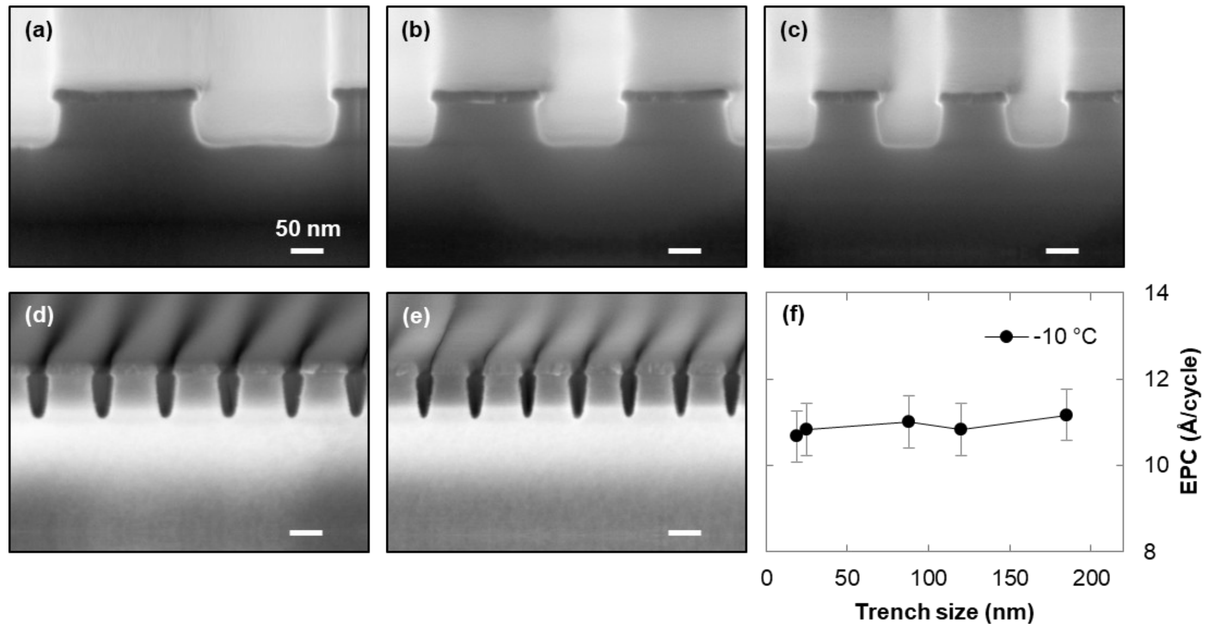

Figure 5. (a) – (e) Cross-sectional SEM images of silicon oxide features patterned using FC-Ar ALE. Experimental parameters are DC bias 9 V, ICP power 300 W, T = -10 °C. Different trench sizes after 60 ALE cycles: 200, 150, 100, 50, 40 nm from (a) to (e). (f) Etching per cycle from nano-sized trenches with electrode temperature at -10 °C. Errors bars indicate the uncertainty from the SEM measurement. Within the errors bars, different feature sizes are all etched at 11 Å/cycles.

Finally, hard mask definition was then carried out using our optimized process after metal lift-off. First, nanoscale features were created using electron-beam lithography on PMMA resist with trenches drawn from 20-200 nm with a mask thickness around 60 nm. E-beam evaporation was then used to deposit 12 nm of Cr at a pressure of 2×10^{-6} Torr. A final lift-off process used to define the Cr lines was performed with Remover PG (MicroChem) followed by acetone cleaning in an ultrasonic bath. **Figure 5(a)-(e)** show the Cr features after being etched for 60 ALE cycles under optimal ALE self-limiting conditions for flat surfaces, *i.e.* DC bias = 9 V, ICP power = 300 W and T = -10 °C, t_{etch} = 60 s. All features present the same vertical profile and a slight undercut is observed. Our process achieved the goal of aspect ratio independent etching. Features with large aspect ratios etch as fast as those with low aspect ratio regardless of feature width. The

slight undercut beneath the mask can be caused by chemical and/or kinetic processes: e.g., ions and radicals reflected from the edges of the feature, broad Ar ions angular distribution, or residual fluorine from the chamber wall.[31] Ions scattered from feature edges can perhaps be ruled out since the sidewall profile does not change significantly with feature width. Regardless of the precise cause, it is clear that in order to achieve features free of undercut and therefore true atomic layer etching, one needs to find a careful balance between the Ar ion parameters (energy and angular distribution) and the fluorocarbon chemical reactant.

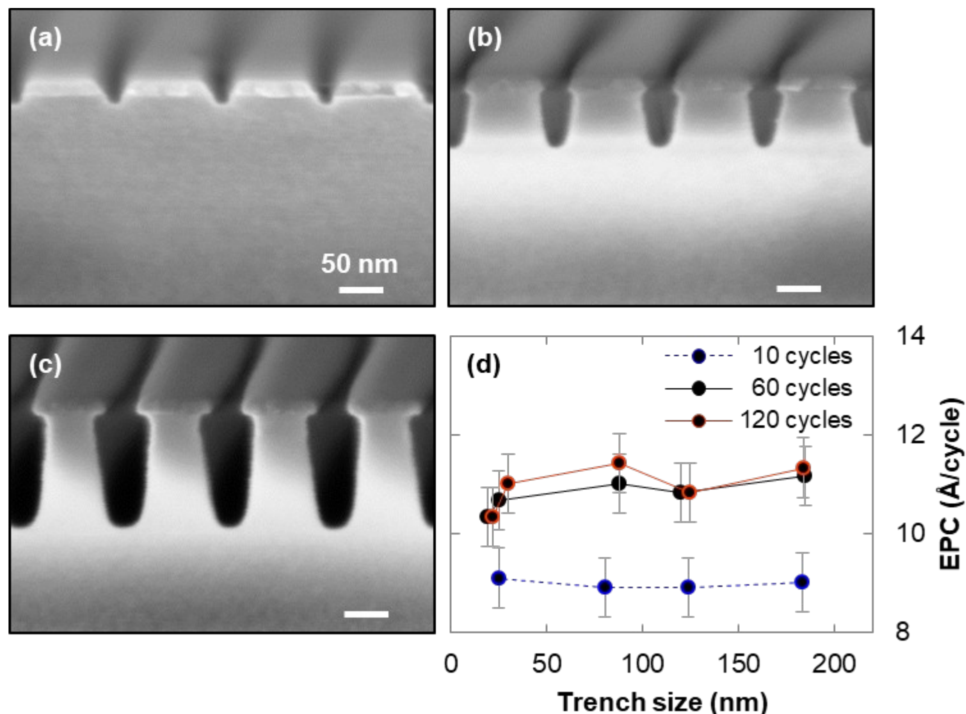

Figure 6. (a)-(c) Cross-sectional SEM images of SiO_2 features patterned using FC-Ar ALE. Experimental parameters are DC bias 9 V, ICP power 300 W, T = -10 °C. Each sample was etched for a varied number of ALE cycles: (a) 10 cycles, (b) 60 cycles and (c) 120 cycles. (d) Etching per cycle from nano-sized trenches under various numbers of cycles. As the trenches are etched deeper, the EPC increases.

We studied the evolution of SiO_2 trench profile over an increasing number of ALE cycles. **Figure 6(a), (b) and (c)** show 30 nm features etched on SiO_2 for 10, 60 and 120 cycles respectively. After 10 ALE cycles, SiO_2 is

etched and the etch depth is approximately 8.5 nm. After 60 ALE cycles, SiO_2 has etched 64 nm (corresponding to an average EPC of 10.7 Å/cycle). Further increasing the number of cycles causes the SiO_2 averaged EPC to remain constant. We clearly observed an increase in the EPC for 60 cycles compared to 10 cycles **(Figure 6(d))**. Other authors have similarly reported a gradual increase in the EPC as a function of the cycle number.[30, 32] It follows that a fluorocarbon film gradually builds up on the reactor walls during each ALE cycle. This fluorocarbon buildup over the course of the sequential ALE cycles provides an additional source of fluorine during the etch step, increasing the EPC.

Notably, the features investigated in Figure 6(c) are 5:1 aspect ratio SiO_2 over Cr trenches. The high selectivity of ALE enables the exposed SiO_2 features to maintain their dimensions while being etched during 120 cycles. The pattern profile shows the successful patterning of silicon dioxide with high selectivity to Cr and the possibility to obtain high aspect ratio-features.

4 Conclusion

In summary, we have shown that by using Ar plasma, periodic injections of CHF_3 and Ar ion bombardment in a conventional plasma tool, atomic layer etching of SiO_2 is possible. Low energy ion bombardment is crucial for minimizing the physical sputtering of SiO_2. This has been studied using a retarding field energy analyzer, and we demonstrated that the Ar ion energies are within the ALE window. A few angstroms of deposited fluorocarbon layer combined with low energy Ar ion bombardment are

used to control the etching of SiO_2. Using ellipsometry, we studied the SiO_2 etch per cycle relative to the etch step time as a function of substrate temperature. At -10 °C the contributions to chemical etching coming from fluorine radicals and fluorocarbon compounds from the chamber walls are minimized and a quasi-self-limiting behavior ALE is observed after 60 s etch time. However, deviation from self-liming ALE behavior and undercut during SiO_2 pattern transfer clearly indicates the presence of a secondary supply of fluorine from the chamber walls. Additionally, during the initial stages of the etch, the fluorocarbon film buildup over multiple ALE cycles causes an increase in EPC with the number of ALE cycles. Future work will be focused on studying the chamber wall chemistry and finding solutions to mitigate its adverse effects. Overall, using ALE at -10 °C we reduced geometric loading effects during etching and reached aspect ratio independent ALE. This type of process enables high flexibility and tunability in terms of precursors, ion energies, fluorocarbon film deposition, substrate temperature, and etch time to further decrease critical dimensions towards the atomic scale pattering era.

Acknowledgments: This work was completed at the Molecular Foundry and supported by the Office of Science, Office of Basic Energy Sciences, of the U.S. Department of Energy under Contract No. DE-AC02-05CH11231. S.D. was supported by Oxford Instruments. We want to thank Matthew Jurow, Michael Elowson, Selven Virasawmy, Scott Dhuey, and Arian Gashi of the Molecular Foundry for their technical support in the cleanroom.

Received:

Revised:

Published online:

Keywords: Atomic layer etching, ion energy distribution, plasma etching, self-limiting process, aspect ratio independent etching

[1] Kuhn K J, Giles M D, Becher D, et al. *IEEE Transactions on Electron Devices* 2011 **58** 2197-2208

[2] Kanarik K J, Tan S and Gottscho R A *The journal of physical chemistry letters* 2018 **9** 4814-4821

[3] Donnelly V M and Kornblit A *Journal of Vacuum Science & Technology A: Vacuum, Surfaces, and Films* 2013 **31** 050825

[4] Lee C G, Kanarik K J and Gottscho R A *Journal of Physics D: Applied Physics* 2014 **47** 273001

[5] Agnello P D *IBM Journal of Research and Development* 2002 **46** 317-338

[6] Kanarik K J, Lill T, Hudson E A, et al. *Journal of Vacuum Science & Technology A: Vacuum, Surfaces, and Films* 2015 **33** 020802

[7] Gottscho R A, Jurgensen C W and Vitkavage D *Journal of Vacuum Science & Technology B: Microelectronics and Nanometer Structures Processing, Measurement, and Phenomena* 1992 **10** 2133-2147

[8] Bailey III A D and Gottscho R A *Japanese journal of applied physics* 1995 **34** 2083

[9] Agarwal A and Kushner M J *Journal of Vacuum Science & Technology A: Vacuum, Surfaces, and Films* 2009 **27** 37-50

[10] Faraz T, Roozeboom F, Knoops H, et al. *ECS Journal of Solid State Science and Technology* 2015 **4** N5023-N5032

[11] Oehrlein G, Metzler D and Li C *ECS Journal of Solid State Science and Technology* 2015 **4** N5041-N5053

[12] Metzler D, Li C, Engelmann S, et al. *Journal of Vacuum Science & Technology A: Vacuum, Surfaces, and Films* 2016 **34** 01B101

[13] Athavale S D and Economou D J *Journal of Vacuum Science & Technology A: Vacuum, Surfaces, and Films* 1995 **13** 966-971

[14] Athavale S D and Economou D J *Journal of Vacuum Science & Technology B: Microelectronics and Nanometer Structures Processing, Measurement, and Phenomena* 1996 **14** 3702-3705

[15] King S W *ECS Journal of Solid State Science and Technology* 2015 **4** N3029-N3047

[16] Schaepkens M and Oehrlein G S *Journal of The Electrochemical Society* 2001 **148** C211-C221

[17] Schaepkens M, Standaert T, Rueger N, et al. *Journal of Vacuum Science & Technology A: Vacuum, Surfaces, and Films* 1999 **17** 26-37

[18] Marra D C and Aydil E S *Journal of Vacuum Science & Technology A: Vacuum, Surfaces, and Films* 1997 **15** 2508-2517

[19] Metzler D, Bruce R L, Engelmann S, et al. *Journal of Vacuum Science & Technology A: Vacuum, Surfaces, and Films* 2014 **32** 020603

[20] Baklanov M R, de Marneffe J-F, Shamiryan D, et al. *Journal of Applied Physics* 2013 **113** 4

[21] Standaert T, Hedlund C, Joseph E, et al. *Journal of Vacuum Science & Technology A: Vacuum, Surfaces, and Films* 2004 **22** 53-60

[22] Kanarik K J, Tan S, Holland J, et al. *Solid State Technology* 2013 **56** 14-17

[23] Gahan D, Dolinaj B and Hopkins M *Review of Scientific Instruments* 2008 **79** 033502

[24] Gahan D, Daniels S, Hayden C, et al. *Plasma Sources Science and Technology* 2011 **21** 015002

[25] Li C, Metzler D, Lai C S, et al. *Journal of Vacuum Science & Technology A: Vacuum, Surfaces, and Films* 2016 **34** 041307

[26] Gottscho R and Kanarik K *Salt Lake City, UT* 2011

[27] Wei T-C and Liu C-H *Surface and Coatings Technology* 2005 **200** 2214-2222

[28] Flamm D, Mogab C and Sklaver E *Journal of Applied Physics* 1979 **50** 6211-6213

[29] Tachi S, Tsujimoto K and Okudaira S *Applied physics letters* 1988 **52** 616-618

[30] Huard C M, Sriraman S, Paterson A, et al. *Journal of Vacuum Science & Technology A: Vacuum, Surfaces, and Films* 2018 **36** 06B101

[31] Gasvoda R J, van de Steeg A W, Bhowmick R, et al. *ACS applied materials & interfaces* 2017 **9** 31067-31075

[32] Lieberman M A and Lichtenberg A J *Principles of plasma discharges and materials processing*: John Wiley & Sons, 2005

Graphical Abstract

Advanced nanomanufacturing requires the ability to achieve atomic scale etching control and material selectivity during pattern transfer. Cyclical fluorocarbon/argon based atomic layer etching satisfied these needs and is here investigated on flat and patterned silicon oxide substrates. Self-limiting behavior is reached by modulating plasma parameters and electrode temperature. Aspect ratio independent etching is demonstrated during the pattern transfer of features.

Stefano Dallorto, Andy Goodyear, Mike Cooke, Julia E. Szornel, Craig Ward, Christoph Kastl, Adam Schwartzberg, Ivo W. Rangelow, Stefano Cabrini*

Atomic Layer Etching of SiO_2 with Ar and CHF_3 Plasmas: a Self-Limiting Process for Aspect Ratio Independent Etching